JOURNAL OF MATERIALS SCIENCE **36** (2001) 3687–3692

Low cost porous mullite-corundum ceramics by gelcasting

YA-FEI LIU, XING-QIN LIU, GANG LI, GUANG-YAO MENG*
Department of Materials Science and Engineering, University of Science and Technology of China, Hefei, Anhui 230026, People's Republic of China
E-mail: mgym@ustc.edu.cn

A gelcasting process has been successfully employed to fabricate porous mullite-corundum ceramic composites from natural clay and corundum powders. The specimens based on the mullite composition are found with an open porosity of 45–47.9%, mean pore size of 1.28–2.55 μm, and nitrogen permeability of 965–5038 $m^3 \cdot m^{-2} \cdot bar^{-1} \cdot hr^{-1}$ by reactively sintering the gelled mixture of kaolinite and α-alumina at 1100–1500°C. The open porosity (ρ_o), mean pore size (d_p), pore size distribution and gas permeability can be controlled by adjusting raw material ratios and sintering temperatures. The gas permeability of the specimens is found to be more dependent on the pore size distribution as well as d_p than on ρ_o. In addition, the gas transportation mechanism in porous mullite-corundum ceramic composites is dominated by viscous flow.

1. Introduction

During the last two decades, mullite ceramics have been developed as advanced electrical, optical, structural, and porous ceramics because of their excellent properties [1–4]. The porous ceramics, however, show more and more successful applications in many fields, such as filters for high-temperature gas purification, filters for molten metals, membranes for separation processes, catalyst carriers for chemical plants and automobiles, and sensors [5]. Specially, hot gas clean-up application by ceramic filters includes such processes as: (a) coal combustion, (b) coal gasification, (c) incineration, (d) catalytic recovery and processing, and (e) chemical and petrochemical processing [6]. Some candidate ceramic materials have been tested with varying degrees of success as the filter and they include silicon carbide, silicon nitride, aluminum oxide, and mullite [7].

The productions of high purity porous mullite ceramics by means of wet chemical routes are usually rather costly and are also limited by their small processing capacities. Using kaolinite as starting material provides a cheaper source, but it also brings some impurities and glassy phases into the products. Therefore, ordinary pottery and porcelain based on clay are limited for porous application because of the production process. The porous corundum ceramics, however, are expensive for their cost and always need very high temperature to be sintered so as to provide enough strength. By combining with the advantages of two or more materials, mullite-based ceramic composites (e.g. cordierite-mullite, alumina-mullite, zirconia-mullite and spinel-mullite) have also been widely investigated [8–10]. Here, porous corundum-mullite ceramics might be an outlet to solve the puzzles.

Ceramic process, particularly the shaping technique has been one of the major activities in ceramic research development. Among the successful techniques, gelcasting is a new shaping route and has been developed since 1990s. It is based on a cross-combined idea from traditional ceramic processing and polymer chemistry. By realizing in-situ polymerization of monomers in a ceramic slurry, it can form complex-shaped and near-net-shaped advanced ceramic materials [11], textured ceramic laminates [12], porous ceramics [13], and ceramic powders [14]. Recently, an automated gelcasting fabrication process was developed to manufacture large-scale ceramic turbine rotors, and the production was reported to be at least 500 rotors per month [15]. Obviously, gelcasting will surely become an important and promising shaping route for production of various-shaped ceramic parts.

In this work, we try to develop this process to prepare porous mullite-corundum ceramics. An investigation on the relationship among phase compositions, microstructure, pore properties and preparation conditions is presented.

2. Experimental procedure

2.1. Specimen preparation

High-purity kaolinite (China Kaolin Company) and α-alumina (Shandong Aluminum Industry Group) were used as the raw materials. The particle size distributions of raw materials powders used in this study were analyzed by a laser analyzer (Coulter LS100, USA), and the mean diameters of kaolinite and α-alumina are 12.06 μm and 16.14 μm, respectively. The mixtures of kaolinite and α-alumina with different ratios were

* Author to whom all correspondence should be addressed.

added into an aqueous solution of organic monomers, monofunctional acrylamide (AM) and difunctional N,N′-methylene-bis-acrylamide (MBAM), and ball-milled. Some dispersants, such as polyaclylic acid (PAA), were added to get a well-dispersed slurry. After initiated by ammonium persulfate and catalyzed by N,N,N′,N′-tetramethylethylenediamine (TEMED), the resulting slurry was molded in a vibrating table. The gelled ceramics were demolded, dried, machined, and then sintered in a programmable high temperature furnace (Nabertherm, Germany) under different temperature from 1100°C to 1500°C for 4 hr.

2.2. Characterizations of the specimens

The compositions of the fired specimens were identified by XRD (Kigaku D/MAz-γ_A rotating X-ray diffraction unit) and their microstructures were observed by SEM (Hitachi X-650 scanning electronic microscope, Japan). The density and open porosity were determined by Archmede's method. The average pore size and pore size distribution of the sintered porous specimens were obtained by the bubble-point method and pure nitrogen flux through the porous disks was measured in a permeation device.

3. Results and discussion

3.1. X-ray diffraction investigations

The gelcasts with different Al_2O_3 wt% were sintered at 1500°C for 4 hr, and the products were identified by XRD in Fig. 1. The specimen made of mere kaolinite (Fig. 1e) shows complete orthorhombic mullite diffraction peaks in addition to the heavy backgrounds, the later reflects the existence of non-crystalline glassy phases due to the decomposition of kaolinite. On the other hand, the sample based on only α-alumina turns out to be corundum entirely at 1500°C (Fig. 1a). For the specimens of their mixtures (Al_2O_3 = 60–80 wt%), however, both mullite and corundum co-existed in the products, and the corundum amount rises as Al_2O_3 wt% increases (Fig. 1b–d). Since 71.8 wt% Al_2O_3 stands for the theoretical composition of mullite, the XRD patterns here show that not all of the alumina reacts with kaolinite and forms secondary mullite. The reason for failing to complete mullitization might be due to using large granular α-alumina (16.14 μm) as raw material.

The green bodies with 71.8 wt% Al_2O_3 were fired at different temperatures for 4 hr separately, and were also identified by XRD. The final phase compositions of the gelcasts depend greatly on the treatment temperatures. Mullite appears at 1100°C, which is mainly the primary mullite derived from the decomposition of kaolinite. When heated at higher temperature, mullite increases steadily in the amount, while corundum monotonously decreases. It means that in addition to the primary mullite, the secondary mullite formed from the reaction between silica (produced from kaolinite) and α-alumina at higher temperature.

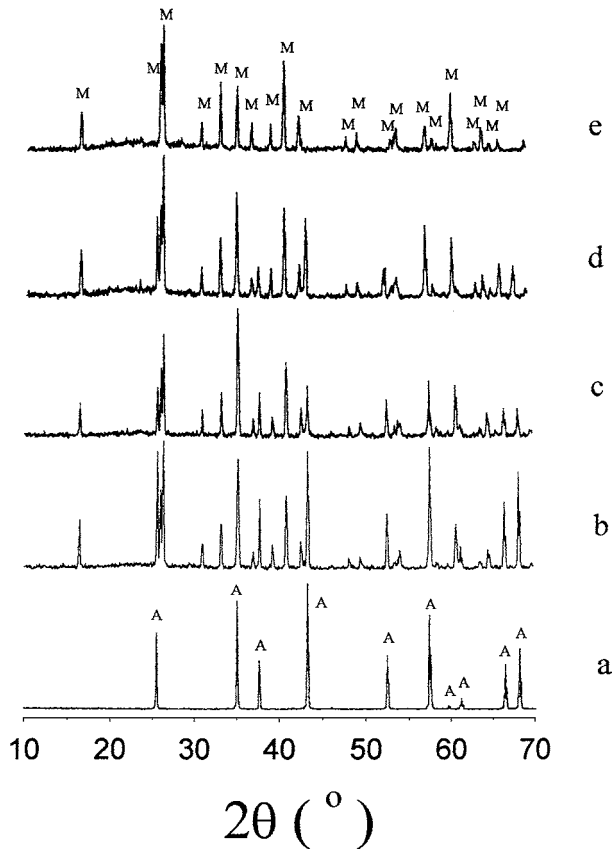

Figure 1 XRD patterns of the specimens with different raw material ratios fired at 1500°C/4hr a-α-alumina; b-80% Al_2O_3 ceramics; c–71.8% Al_2O_3 ceramics; d-60% Al_2O_3 ceramics; e-Kaolinite M-Mullite, A-Corundum.

3.2. Pore parameters of sintered specimens

3.2.1. Porosity

The effects of the preparation conditions (e.g. the sintering temperatures, the raw material ratios) on the open porosity of the fired specimens were illustrated in Fig. 2. For the gelcast made of kaolinite (~43.7wt% Al_2O_3) alone, the open porosity (ρ_o) depends more closely on the sintering temperature than those made of the mixtures of kaolinite and α-Al_2O_3. The kaolinite specimen shows the largest sintering shrinkage due to forming large amount of glassy phase and thus is the sample with the lowest porosity (ρ_o = 8.6–41.4%) at

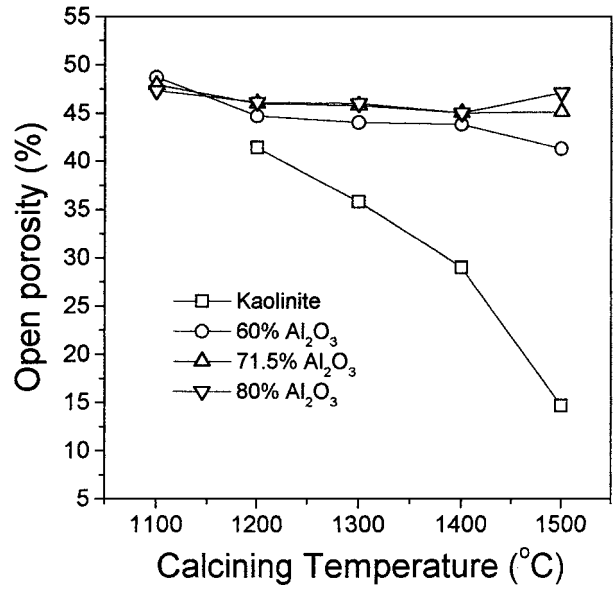

Figure 2 Open porosity of the specimens fired at different temperatures.

any heating temperatures. On the contrary, the calcining temperature doesn't bring too much influence on the open porosity for the mixture specimens with 60–80 wt% Al_2O_3, especially for the gelcast with mullite composition (71.8 wt% Al_2O_3, $\rho_o = 45$–47.9%). The 60% Al_2O_3 sample undergoes a slight drop in ρ_o over 1400°C, which suggests that kaolinite still affects the pore distribution and might cause some closed pores in the system when $T \geq 1400$°C. On the other hand, the 80% Al_2O_3 sample gets a little rise in ρ_o over 1400°C, which hints that less kaolinite in the system might reduce the existence opportunity for closed pores at higher temperature.

3.2.2. Pore size distributions and average pore sizes

The pore size distributions of the mullite-corundum ceramics (~71.8 wt% Al_2O_3) are closely related to the sintering temperatures (Fig. 3). The average pore size (d_p) rises with the sintering temperature, and the d_p values are 1.28, 1.70, 1.95 and 2.55 μm for 1100, 1250, 1300 and 1500°C, respectively. In the meantime, pore size distribution scopes extend from 1.2 μm to 3 μm, though there are little changes in the open porosity of the 71.8% Al_2O_3 sample treated between 1100–1500°C according to Fig. 2. As we know, ρ_o can only tell open pores from closed pores, so the pore-enlarging trend might be caused by two possible reasons: (a) the liquid glassy phases (mainly silica) flow, react with α-Al_2O_3, and form big pores; (b) some small open pores merge with each others and lead to big open pores, accompanying with nearly no change in closed pores. For all specimens, the pore size distributions are within a very narrow range of 1.0–4.5 μm, which is a favorable result for a porous material.

The raw material ratios also have influence on the pore size distributions of the ceramic composites fired at 1500°C for 4 hr, as shown in Fig. 4. As Al_2O_3% rises, d_p increase gradually, and its values of the specimens

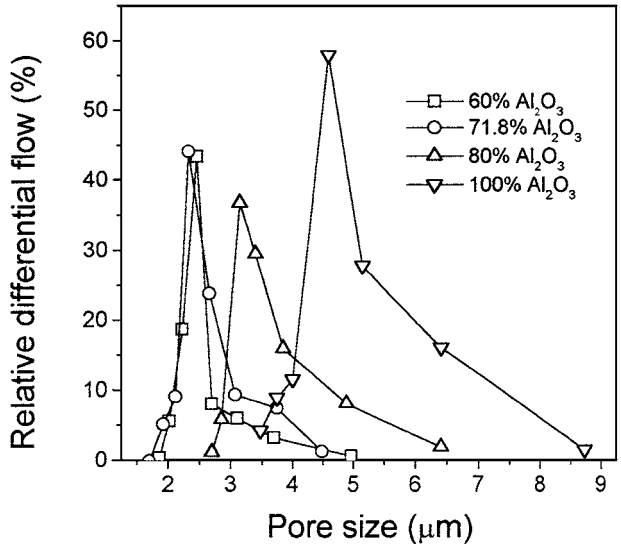

Figure 4 Pore size distributions of the specimens with different raw material ratios fired at 1500°C for 4 hr.

with 60%, 71.8%, 80% and 100% Al_2O_3 are 2.31 μm, 2.55 μm, 3.49 μm and 4.99 μm, respectively. The pore size distribution curves of 60% and 71.8% Al_2O_3 coincide with each other, so there might be similar pore structure for them. Both of them are ascribable to the existence of dominant glassy silica phases, which formed from the decomposition of kaolinite at around 1000°C and diffused into the small openings produced by burnout of the cross-linked polymer network. High Al_2O_3 % specimens, however, provide more alumina to react with the glassy silica and thus raises the pore size.

3.2.3. Gas permeability

Fluid permeability is an important parameter for a porous ceramics. The nitrogen fluxes of the same specimens as presented in Fig. 3 are illustrated in Fig. 5. The flux goes up with the pressure drop and sintering temperature, its values are 965, 1740, and 5038 $m^3 \cdot m^{-2} \cdot bar^{-1} \cdot hr^{-1}$ for 1100, 1300, and 1500°C, respectively. The flux change trend is in agreement with that of

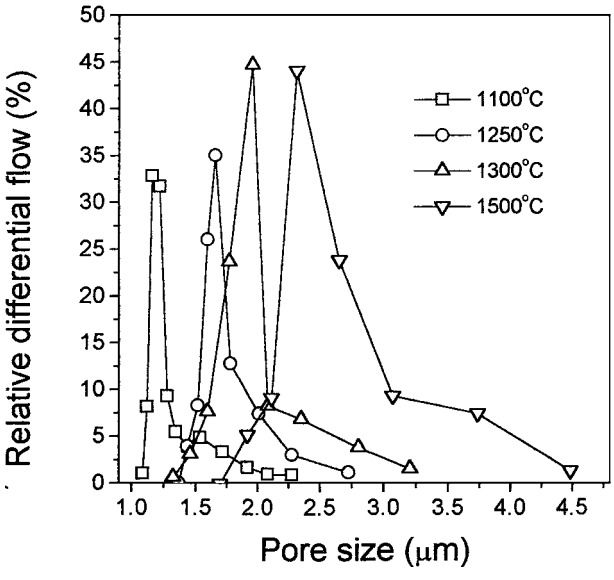

Figure 3 Pore size distributions of the 71.8 wt% Al_2O_3 specimens fired at different temperatures.

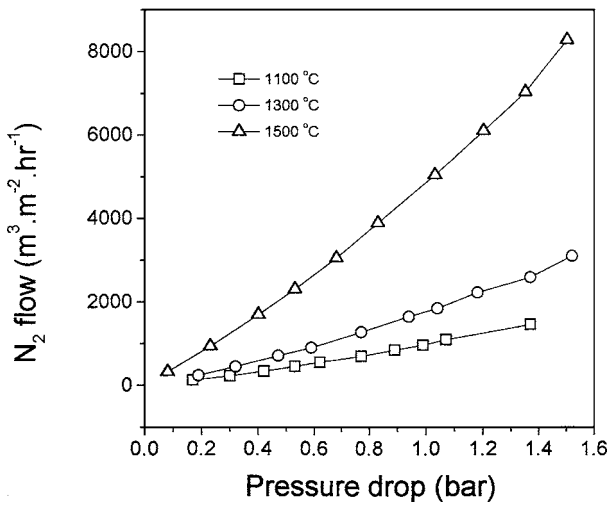

Figure 5 Nitrogen fluxes of the 71.8 wt% Al_2O_3 specimens fired at different temperatures for 4 hr.

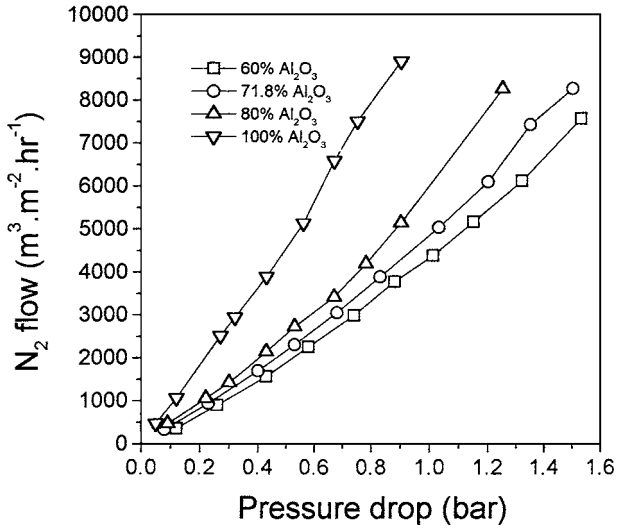

Figure 6 Nitrogen fluxes of the specimens with different raw material ratios fired at 1500°C/4 hr.

mean pore sizes in Fig. 3, but not similar to that of open porosity in Fig. 2. These seem as if flux were mainly affected by mean pore size. However, from Fig. 5, we find big flux change (∼1.89 times) when the firing temperature rises from 1300 to 1500°C, while there is only about 30.8% increase for d_p values. According to Fig. 3, the pores bigger than 3.0 μm take up well enough proportion at 1500°C, and thus have the weather gauge of gas flux against that of 1300°C. Therefore, it is the pore size distribution that brings influence on the gas flux. As we know from related XRD patterns, much more mullite is formed when the specimen is fired at 1500°C than 1300°C, so the pore size distribution is a result of both the phase compositions and microstructure.

Fig. 6 illustrates the nitrogen fluxes of the specimens with different Al_2O_3% fired at 1500°C for 4 hr. The gas flux increases with the pressure drop as well as Al_2O_3%, and its values are 4341, 4891, 5709 and 9882 $m^3 \cdot m^{-2} \cdot bar^{-1} \cdot hr^{-1}$ for 60%, 71.8%, 80% and 100% Al_2O_3 ceramic specimens, respectively. The flux change trend for most ceramic specimens agrees well with that of mean pore size (Fig. 4) and open porosity (Fig. 2), and the gas fluxes of the mullite-corundum ceramics made of gelcasts with 60–80% Al_2O_3 come close to each other compared with the corundum ceramic.

It is very interesting that the N_2 fluxes do not show liner dependence of pressure drop in both of Fig. 5 and Fig. 6. Therefore, there might be special gas permeability mechanism underlying it, which will be explained in Sect. 3.4.

3.3. SEM of the specimens

The SEM photographs of the fracture surfaces of the gelcasts fired at 1500°C for 4 hr are shown in Fig. 7. Fig. 7a displays the morphology of the specimen based on mere kaolinite, a large quantity of continuous glassy phases remains in the reaction system, in which some small and big pores are embedded. Referring to Fig. 1e, the main phase in Fig. 7a should be mullite, and the latter forms the sketch of the glassy phases. At a temperature as high as 1500°C, the glassy phases are less viscous and easy to flow, so they can fill most pores formed by burn-out of the gelled polymer and thus drop the open porosity dramatically (c.f. Fig. 2). Fig. 7b indicates the case of the gelcast with 71.8% Al_2O_3, most of the pore sizes are around 1–5 μm, affirming to the measurement results in Fig. 4. The photograph of more alumina specimen (e.g. 80% Al_2O_3) is shown in Fig. 7c, kaolinite is less than α-alumina in the raw material ratio, it exists at the gaps of α-alumina at the beginning, and then forms pores due to the reaction between corundum and glassy silica at high temperature. For the specimen produced completely from α-alumina (Fig. 7d), the large pores form from the piling effect of the raw material with big granule sizes. The big particles seem not fully sinter with each other, on which the tiny grains might be brought by the raw material. Thus, this specimen fails to provide enough mechanical strength.

3.4. Mechanism of gas permeability

In general, when a gas flows through a porous medium, its possible transport mechanisms are viscous or Poiseuille flow, molecular flow or Knudsen diffusion. It is found that in isothermal gas phase transport under a pressure gradient, viscous flow and Knudsen diffusion become more important than molecular diffusion. So, the permeability can usually be represented by [16]:

$$F_o = \frac{J}{\Delta P} = C_1 + C_2 P_m \qquad (1)$$

where F_o is the permeability ($mol \cdot m^{-2} \cdot s^{-1} \cdot Pa^{-1}$), J the flux ($mol \cdot m^{-2} \cdot s^{-1}$), ΔP the pressure drop (Pa), P_m the average pressure in the porous material (Pa), C_1 and C_2 two constants representing Knudsen diffusion and viscous flow respectively.

According to Equation 1, it can be understood why nonlinear relationships appear between the N_2 flux and pressure drop ΔP as shown in Fig. 5 and Fig. 6, if the permeability is not just controlled by Knudsen diffusion (C_1), but also by viscous flow (C_2). The plots of permeability in the mullite-corundum ceramics versus mean pressure are illustrated in Fig. 8. It is found that good linear relationships exist between F_o and P_m for the specimens with nominal mullite composition fired at different temperatures. The values of C_1 and C_2 for each temperature can be obtained by fitting the plots into straight lines, and the results are listed in Table I. Both C_1 and C_2 increase as the firing temperature rises, but the values of C_2 are remarkably larger than those of C_1. It suggests that viscous flow (laminar flow) take more effect than Knudsen diffusion for the gelcasted

TABLE I The diffusion constants of the gelcasts fired at different temperatures

Temperature (°C)	1100	1300	1500
C_1	16.15	21.10	216.5
C_2	703.6	1309.4	2590.6

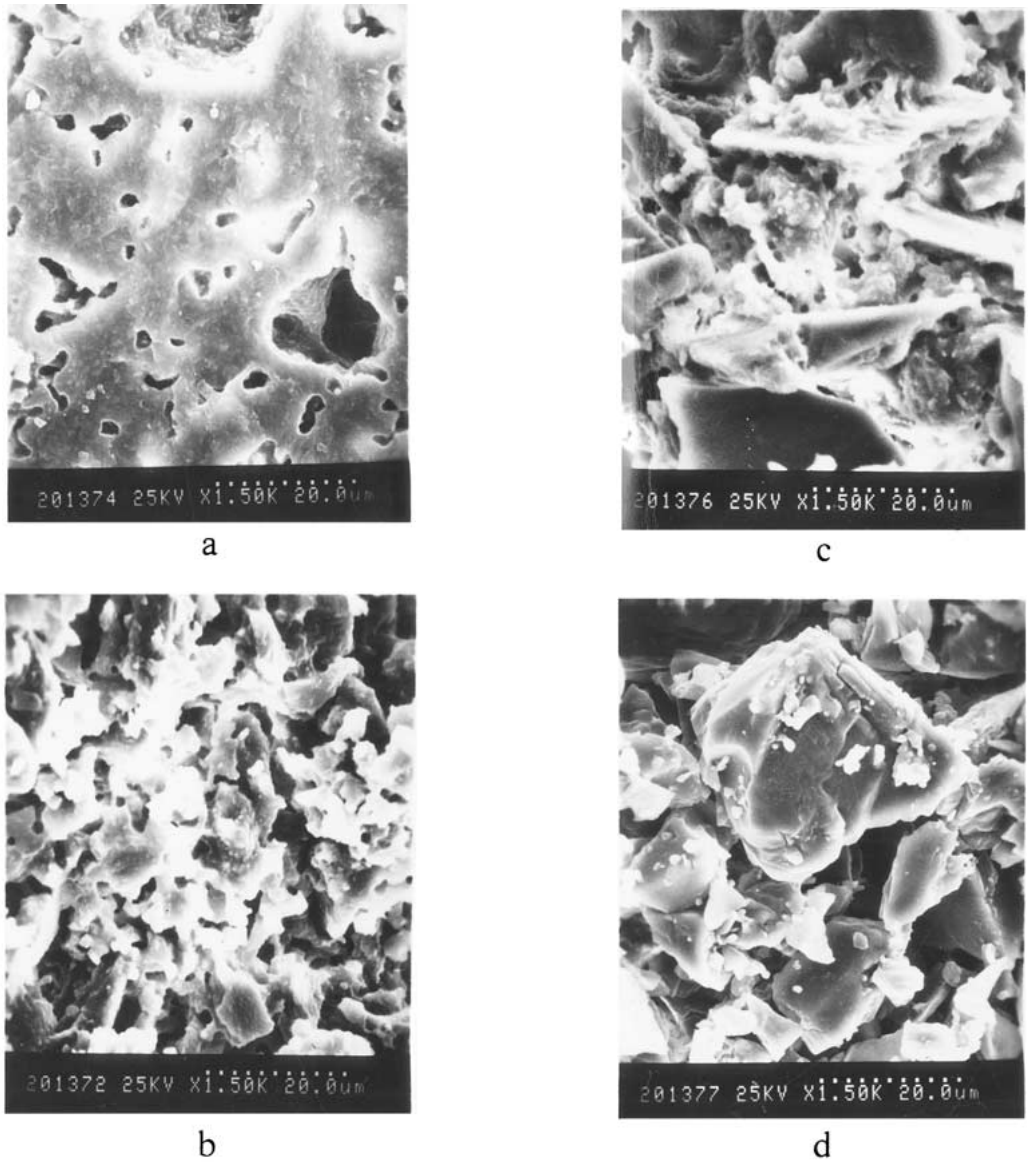

Figure 7 SEM photographs of the fracture surfaces of gelcasted ceramics fired at 1500°C/4 hr a-Kaolinite; b-71.8% Al_2O_3 ceramics; c-80% Al_2O_3 ceramics; d-α-alumina.

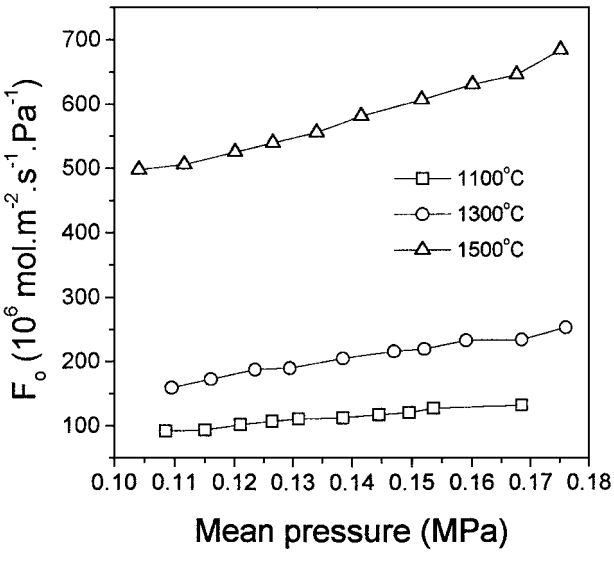

Figure 8 Plots of permeability in the mullite-corundum ceramics versus mean pressure.

71.8% Al_2O_3 specimens at the temperature range of 1100–1500°C.

As we see from Fig. 3, the mean pore sizes for the specimens fired at 1100–1500°C are around 1.28–2.55 μm, which are rather bigger than the mean free path of N_2 molecule (~50 nm), so they can't well meet the condition of Knudsen diffusion. Moreover, the pore size distribution for 1500°C specimen is much broader than specimens made at lower temperatures, and more big pores appear for the high-temperature samples. There should not be much Knudsen diffusion at 1500°C, the abnormal increase in C_1 from 1300–1500°C is still unclear, which needs further investigations. On the other hand, viscous flow is attributed to those big pores, and it dominates the gas diffusion with the increasing sintering temperature.

4. Conclusions

1. Gelcasting process has been successfully employed to fabricate porous mullite-corundum ceramic composites.

2. The properties of porous mullite-corundum ceramics such as porosity, average pore size, pore size distribution and gas flux can be controlled by adjusting the preparation conditions (e.g. raw material ratio and sintering temperature). The open porosity, average pore size and nitrogen flux of the mullite ceramics ($\sim$71.8 wt% Al_2O_3) sintered at 1100–1500°C are around 45–47.9%, 1.28–2.55 μm, and 965–5038 $m^3 \cdot m^{-2} \cdot bar^{-1} \cdot hr^{-1}$, respectively. The mean pore sizes are related to both of the glassy-phase-lessening and alumina particle size.

3. The gas permeability of the specimens is more dependent on pore size distribution as well as d_p than open porosity. The gas transportation in porous mullite ceramics is affected by both of Knudsen diffusion and viscous flow, and it is dominated by the latter.

Acknowledgements

The authors would like to thank the Natural Science Foundation of China and Natural Science Foundation of Anhui Province for their firmly financial support.

References

1. I. H. AKSAY, D. M. DABBS and M. SARIKAYA, *J. Amer. Ceram. Soc.* **74**(10) (1991) 2343.
2. H. SCHNEIDER and E. EBERHARD, *ibid.* **73**(7) (1990) 2073.
3. H. SCHNEIDER, M. SCHMUCKER, K. IKEDA *et al.*, *ibid.* **76**(11) (1993) 2912.
4. R. A. TERPSTRA, B. C. BONEKAMP and H. J. VERINGA, *Desalination* **70** (1988) 395.
5. P. SEPULVEDA, *Am. Ceram. Soc. Bull.* **76**(10) (1997) 61.
6. J. F. ZIEVERS, E. C. ZIEVERS and P. EGGERSTEDT, *AIChE National Meeting*, Chicago, IL (Nov. 12–16, 1990)
7. P. M. EGGERSTEDT, J. F. ZIEVERS and E. C. ZIEVERS, *Chem. Engineer. Prog.* **1** (1993) 62.
8. M. G. M. U. ISMAIL, H. TSUNATORI and Z. NAKAI, *J. Amer. Ceram. Soc.* **73**(7) (1990) 537.
9. P. BOCH and T. CHARTIER, *ibid.* **74**(10) (1991) 2448.
10. M. SALES, C. VALENTIN and J. ALARCON, *J. Sol-Gel Sci. Technol.* **8** (1997) 871.
11. A. C. YOUNG, O. O. OMATETE, M. A. JANNEY, *et al.*, *J. Am. Ceram. Soc.* **74**(3) (1991) 612.
12. D. M. BASKIN, M. H. ZIMMERMAN and K. T. FABER, *ibid.* **80**(11) (1991) 2929.
13. H. T. WANG, X. Q. LIU and G. Y. MENG, *Mater. Res. Bull.* **32**(12) (1997) 1705.
14. H. T. WANG, S. XIE, W. LAI *et al.*, *J. Mater. Sci.* **34**(6) (1999) 1163.
15. G. GEIGER, *Am. Ceram. Soc. Bull.* **78**(5) (1999) 20.
16. R. J. R. UHLHORN, M. H. B. J. HUIS IN'T VELD, K. KEIZER, *et al.*, *J. Mater. Sci.* **27** (1992) 527.

Received 14 June
and accepted 20 December 2000